Chemical Science

ROYAL SOCIETY OF CHEMISTRY

EDGE ARTICLE

View Article Online
View Journal

Cite this: DOI: 10.1039/d6sc00432f

All publication charges for this article have been paid for by the Royal Society of Chemistry

Regioselective synthesis of aza-saccharins *via* anionic [1,4] Fries-type rearrangement of aryl sulfonimidoyl fluorides

Mario Leypold, *[a] Lorenzo Poli, [a] Max Earl, [a] Okky D. Putra, [b] Karolina Kwapien, [a] Richard J. Lewis, [a] John J. Murphy, [a] Marta Passamonti, [a] Lena M. von Sydow, [a] Victor Spelling, [c] Ioannis Asproudis, [b] Malvika Sardana, [c] Claudia Gatti, [d] Hikaru Seki, [a] Thomas Lemaitre, [a] Radvile Juskaite, [a] Ranganath Gopalakrishnan, [a] Stuart J. Francis, [a] Cristina Gardelli, [a] Per-Ola Norrby [e] and Werngard Czechtizky [a]

A regioselective synthesis of aromatic and aliphatic aza-saccharins as cyclic sulfonimidamide derivatives is reported, starting from easily accessible aryl sulfonimidoyl fluorides and primary or secondary amines with broad functional group tolerance. The transformation is enabled by electron-withdrawing substituents and proceeds through an anionic [1,4] Fries-type rearrangement at cryogenic temperature, initiated by KHMDS-mediated *ortho*-deprotonation and rapid carbonyl migration. Mechanistic investigations indicate the formation of aryl sulfonimidoyl fluoridate anions, a distinct and previously unexplored motif in S(VI) and SuFEx chemistry. The involvement of these low-temperature-persistent intermediates is supported by cryogenic $^{19}F/^{15}N$ NMR studies of a ^{15}N-labeled substrate, interception by acylation to give a stable adduct whose structure was confirmed by X-ray diffraction, and complementary DFT calculations indicating that the fluoridate anion is a viable low-energy intermediate. Regioselectivity follows predictable electronics-driven trends governed by *meta*-substituents, while selective aza-saccharin formation can be modulated by base choice and reagent addition order. Notably, the fluoridate anions are configurationally stable at sulfur, as demonstrated in a representative example, and subsequent amination *via in situ* SuFEx capture proceeds stereospecifically with inversion at sulfur. This synthetic method provides a mechanistically defined and stereocontrolled entry to chiral aza-saccharins with potential relevance to medicinal chemistry, agrochemical discovery and related disciplines.

Received 15th January 2026
Accepted 16th April 2026

DOI: 10.1039/d6sc00432f

rsc.li/chemical-science

Introduction

Within the pharmaceutical industry, medicinal chemists are confronted with the continuous task of improving the properties of bioactive compounds while simultaneously balancing efficacy with safety and tolerability. In their pursuit, a promising class of compounds known as sulfonimidamides has emerged as bioisosteric substitutes for widely used sulfonamides, thanks to their favorable blend of physicochemical and pharmacokinetic characteristics.[1–3] These features have positioned sulfonimidamides as compelling motifs for addressing limitations associated with established sulfur(VI)-based scaffolds and for enabling therapeutic innovation. As a result, sulfonimidamides have attracted significant attention, leading to multiple patents since 2018 that highlight their utilization as inhibitors for NLRP-,[4] STING-,[5] and LXR-related disorders,[6] and their potential for pesticidal applications.[7]

In the realm of sulfonimidamides, an additional level of structural complexity can be achieved through rigidification in the form of cyclic analogs. Among these structures, aza-saccharins stand out as three-dimensional heterocycles with amine exit vectors positioned out of the plane, offering opportunities for diversification. Despite this promise, general synthetic access to aza-saccharins remains limited in the open literature. To date, our laboratories have disclosed the single general method for their synthesis relying on the ring closure of *tert*-butyldimethylsilyl-protected (TBS-protected) acyclic aryl sulfonimidamides onto a pre-installed ester moiety in *ortho*-position (Scheme 1A).[8] According to our survey of the literature,

[a]*Medicinal Chemistry, Research and Early Development, Respiratory and Immunology, BioPharmaceuticals R&D AstraZeneca, Pepparedsleden 1, 43183 Mölndal, Sweden. E-mail: mario.leypold@astrazeneca.com*

[b]*Early Product Development and Manufacturing, Pharmaceutical Sciences, R&D AstraZeneca, Pepparedsleden 1, 43183 Mölndal, Sweden*

[c]*Early Chemical Development, Pharmaceutical Sciences, R&D AstraZeneca, Pepparedsleden 1, 43183 Mölndal, Sweden*

[d]*Early Chemical Development, Pharmaceutical Sciences, R&D AstraZeneca, Macclesfield SK10 2NA, UK*

[e]*Predictive Science, Digital and Automation, Pharmaceutical Sciences, R&D AstraZeneca, Pepparedsleden 1, 43183 Mölndal, Sweden*

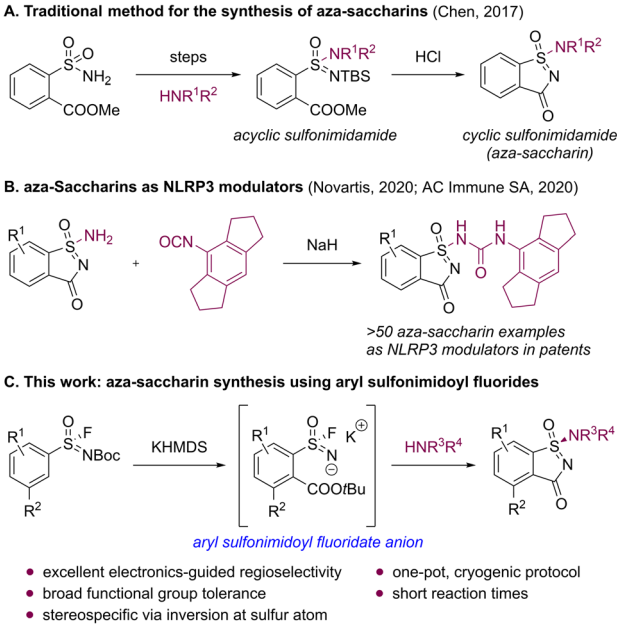

Scheme 1 Methods for the synthesis of aza-saccharins and applications.

this methodology was subsequently applied in 2020 patent disclosures, which describe the only additional examples of aza-saccharins, encompassing over 50 compounds evaluated as NLRP3 modulators (Scheme 1B).[9,10] Given our interest in aza-saccharins for fragment-based hit finding and to broaden the synthetic access to this compound class, we developed an orthogonal strategy for the synthesis of aza-saccharins that employs an anionic [1,4] Fries-type rearrangement[11,12] of aryl sulfonimidoyl fluorides, followed by sulfur(VI) fluoride exchange (SuFEx) chemistry.[1u,13] The transformation proceeds *via* cryogenically stable aryl sulfonimidoyl fluoridate anions, which, to the best of our knowledge, have not been previously reported as intermediates or reactive motifs in SuFEx processes, and are intercepted *in situ* by amines to effect ring closure (Scheme 1C). The involvement of these fluoridate anions is supported by cryogenic $^{19}F/^{15}N$ NMR studies of a ^{15}N-labeled substrate, acylation trapping with X-ray characterization of a resulting adduct, and complementary computational simulations. In this study, we describe the regioselective synthesis of substituted aza-saccharins with its applicability to stereospecific protocols using easily accessible *tert*-butyloxycarbonyl-protected (Boc-protected) aryl sulfonimidoyl fluorides and amines with broad functional group tolerance.

Results and discussion

Reaction optimization

During our investigation into the formation of acyclic sulfonimidamides, we discovered a novel reactivity pattern upon the addition of potassium bis(trimethylsilyl)amide (KHMDS) to a solution containing sulfonimidoyl fluoride **1a** and 2-aminopyrimidine (**2a**), resulting in the concomitant formation of aza-saccharin **3a** and acyclic sulfonimidamide **4a**. We hypothesized that favorable aza-saccharin formation could be facilitated by KHMDS pre-activation (KPA) of sulfonimidoyl fluoride **1a**, which induces an anionic [1,4] Fries-type rearrangement to an ester analogue in *ortho*-position,[14] akin to our previously established route (Scheme 1A), prior to the addition of amine. Under optimized reaction conditions, the treatment of sulfonimidoyl fluoride **1a** (1 equiv.) with KHMDS (2.00 equiv.) at −78 °C, followed by the addition of 2-aminopyrimidine (**2a**, 1.20 equiv.), resulted in quantitative conversion and high isolated yield of aza-saccharin **3a** (Table 1, Entry 1).[15] Deviations from the optimized conditions revealed pronounced sensitivity to solvent, substrate structure, protecting group, reagent addition order, as well as base identity and equivalents. Among the ethers examined, tetrahydrofuran (THF) proved most effective, whereas methyl *tert*-butyl ether (MTBE) gave the lowest LCMS yield (Entry 2).[16] Furthermore, the sulfonimidoyl chloride analogue of sulfonimidoyl fluoride **1a** failed to furnish detectable aza-saccharin **3a** and instead led to substrate degradation (Entry 3).[17] In contrast, the methoxycarbonyl-protected (Moc-protected) aryl sulfonimidoyl fluoride still afforded the corresponding aza-saccharin **3a**, albeit with diminished LCMS and isolated yields accompanied by increased side product formation (Entry 4).[18] When KHMDS was added in the presence of amine **2a**, preferential formation of acyclic sulfonimidamide **4a** was observed (Entry 5). Interestingly, silazide bases with more Lewis-acidic counterions, such as lithium bis(trimethylsilyl)

Table 1 Optimization of reaction conditions for aza-saccharin formation[a]

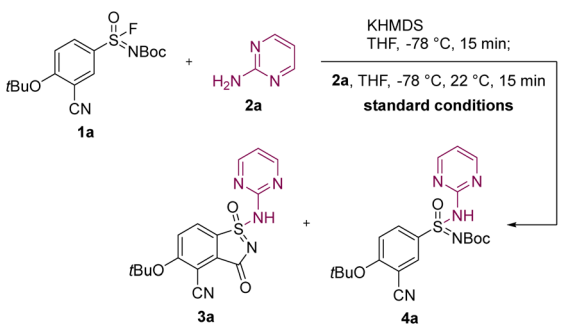

Entry	Deviation from standard conditions	LCMS yield **3a**, [**4a**] (%)[b]
1	None	>99 {89}[c], [n.d.]
2	MTBE[d]	81, [7]
3	Sulfonimidoyl chloride	Degradation
4	Moc	68 {52}[c], [n.d.]
5	KHMDS (2.00 equiv.) added last	6, [92]
6	LiHMDS (2.00 equiv.)	2, [95]
7	NaHMDS (2.00 equiv.)	91, [n.d.]
8	KHMDS (1.50 equiv.)	82, [n.d.]
9	KHMDS (2.50 equiv.)	84, [n.d.]

[a] Reaction conditions: sulfonimidoyl fluoride **1a** (75.0 μmol, 1 equiv.), KHMDS (150 μmol, 2.00 equiv.), THF, −78 °C, 15 min; 2-aminopyrimidine (**2a**, 90.0 μmol, 1.20 equiv.), THF, −78 °C, 22 °C, 15 min. [b] LCMS yield of Entry 1 verified *via* NMR experiment with 1,3,5-trimethoxybenzene as internal standard. [c] Isolated yield on a 400 μmol scale. [d] KHMDS (1 M in THF) used. n.d. = not detected.

amide (LiHMDS) or sodium bis(trimethylsilyl)amide (NaHMDS),[19,20] were found to be less reliable in the pre-activation of sulfonimidoyl fluoride **1a** (Entries 6 and 7). While the origin of this counterion dependence is not fully established, it may reflect differences in ion pairing, aggregation and/or metal–substrate coordination of alkali-metal silazides under cryogenic conditions.[21] Collectively, the strong dependence on reagent addition order and on the alkali-metal silazide employed provides a practical handle to control the chemoselectivity in the synthesis of aza-saccharins and acyclic sulfonimidamides. Finally, the optimized amount of KHMDS proved essential for achieving ideal results in aza-saccharin synthesis (compare Entries 1, 8 and 9).[22]

Substrate scope

The synthetic application of this chemistry to aza-saccharin formation was investigated using aryl sulfonimidoyl fluorides and their corresponding aza-saccharins (Scheme 2), while heteroaryl analogues were not examined. Various inductive electron-withdrawing substituents in the *meta*-position relative to the sulfonimidoyl fluoride moiety were compatible, and provided aza-saccharins **3** with complete (**3b–3g**) or high regioselectivity (**3h** : **3h′** = 92 : 8). Notably, cyclization in these substrates occurred at the sterically more demanding reaction site. Electron-withdrawing substituents in the *para*-position yielded aza-saccharins **3i–3k** in fair yields, while *ortho*- and unsubstituted aza-saccharins **3l**, **3m** required higher temperatures due to less efficient KPA in the corresponding sulfonimidoyl fluorides under standard conditions.

The use of bis-*meta*-substituted sulfonimidoyl fluorides enabled the synthesis of the corresponding aza-saccharins **3n–3r**, and allowed mapping of relative cyclization trends based on observed regioselectivities influenced by substituents in the *meta*-position. The KPA of sulfonimidoyl fluorides appears to be governed by both inductive effects and polarization contributing to acidification, and potential stabilization of carbanions *via* negative hyperconjugation (*vide infra*).[23] Leading to a productivity trend for substituents in the aza-saccharin synthesis of F > SOFNBoc > Cl ~ Br ~ CN > CF_3 > H,[20,24,25] these observations align better with the reactivity and regioselectivity patterns observed in the deprotonation of substituted arenes using strong potassium bases,[26] yet complementary to the directed *ortho*-metalation with chelating lithium reagents.[27]

A limitation of the methodology was observed for aryl sulfonimidoyl fluorides bearing electron-donating substituents or extended π-systems. Under standard conditions, the 4-methoxy and 2-naphthyl derivatives failed to afford aza-saccharins **3s**, **3t**, respectively.[20,28] These results indicate that reactivity under the current KPA conditions may require substrate-specific reoptimization, beyond the temperature adjustment used for less activated aryl sulfonimidoyl fluorides (aza-saccharins **3l**, **3m**).

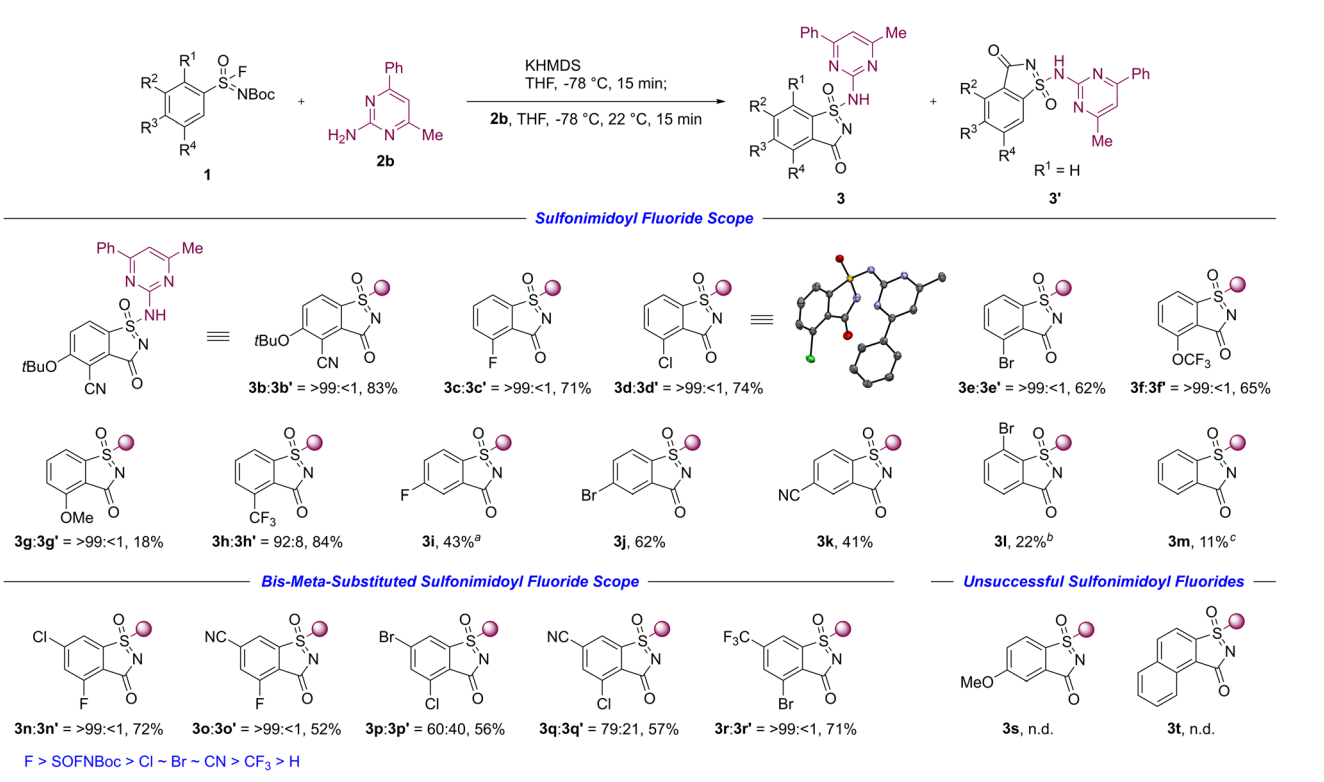

Scheme 2 aza-Saccharin formation: scope of aryl sulfonimidoyl fluorides. Reaction conditions: sulfonimidoyl fluoride **1** (400 μmol, 1 equiv.), KHMDS (800 μmol, 2.00 equiv.), THF, −78 °C, 15 min; 4-Me-6-Ph-pyrimidine-2-amine (**2b**, 480 μmol, 1.20 equiv.), THF, −78 °C, 22 °C, 15 min. [a]KPA: −78 °C, 4 h. [b]KPA: −50 °C, 15 min. [c]KPA: −30 °C, 30 min. Values correspond to isolated yields for the mixture of regioisomers. Displacement ellipsoids are drawn at the 50% probability level. Hydrogen atoms and minor parts are omitted for clarity. n.d. = not detected (below LCMS detection limit in reaction mixture).

The substrate scope exploration encompassing a wide range of amines and other nitrogen nucleophiles is presented in Scheme 3. 6-membered and 5-membered primary aromatic amines bearing heteroatom-substituted and sterically hindered motifs were tolerated to provide the corresponding aza-saccharins **3a**, **3u–3ab** in 54−90% yields. Of particular significance, the synthesis of aza-saccharin **3a** could be readily accomplished on a 2.00 mmol scale without compromising the efficiency of the reaction. Importantly, this transformation displayed high functional group tolerance to enable direct access to functionalized aza-saccharins **3ac–3ah**, even in the presence of acidic α-protons relative to the silazide base added, such as demonstrated in ketone- **3ai**, lactam- **3aj**, sulfone- **3ak**, and phosphine oxide-containing aza-saccharin **3al**. The successful formation of aza-saccharin **3am** in 40% yield additionally expands the applicability of this methodology to secondary aromatic amines as reaction partners.

Initially, aliphatic amines compromised the desired aza-saccharin formation. During the KPA of sulfonimidoyl fluorides, the silazide anion functioned exclusively as a base. However, at temperatures above −78 °C, it additionally displayed dual reactivity and acted as a nucleophile in the SuFEx reaction, leading to competition with aliphatic amines due to similar nucleophilicity in contrast to aromatic amines. To mitigate side product formation, a modified protocol was developed by increasing the amount of aliphatic amine added (2.00 equiv., Scheme 3). This modification proved effective, resulting in the synthesis of aza-saccharins **3an–3at** in 20−53% yields.[29] The free amino analogue aza-saccharin **3au** was obtained in 56% yield using KHMDS directly as an NH_2 surrogate. This orthogonal approach would allow access to additional regioisomers of the previously reported NLRP3 modulators when combined with the isocyanate-based modification described above (*cf.* Schemes 1B and 2). Furthermore, the successful isolation of aza-saccharin **3av**, utilizing morpholine as a reaction partner, demonstrates the applicability of this synthetic protocol to secondary aliphatic amines.

In addition to aromatic and aliphatic amines, a set of other nitrogen nucleophiles was evaluated under the standard conditions. A representative hydrazine and sulfonamide did not furnish the corresponding aza-saccharins **3aw**, **3ax**, and instead led to notable side product formation. Selected mono-aza

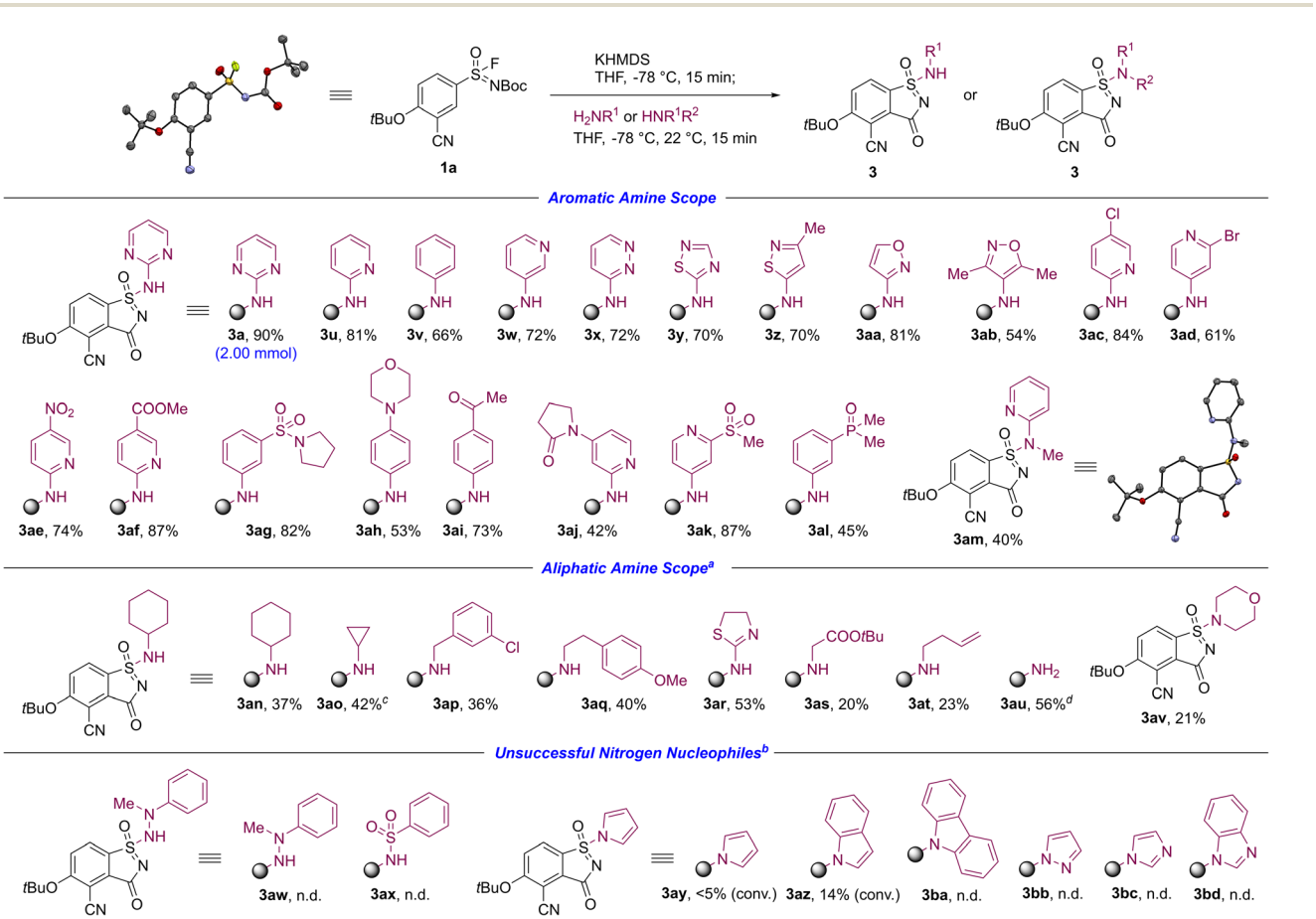

Scheme 3 aza-Saccharin formation: scope of amines and nitrogen nucleophiles. Reaction conditions: sulfonimidoyl fluoride **1a** (400 μmol, 1 equiv.), KHMDS (800 μmol, 2.00 equiv.), THF, −78 °C, 15 min; amine **2** (480 μmol, 1.20 equiv.), THF, −78 °C, 22 °C, 15 min. [a]For aliphatic amines: amine **2** (800 μmol, 2.00 equiv.). [b]Nitrogen nucleophiles investigated on a 100 μmol scale with LCMS conversions reported. [c]After amine addition: 0 °C, 15 min. [d]KHMDS as NH_2 surrogate: 40 °C, 2 h. Values correspond to isolated yields. Displacement ellipsoids are drawn at the 50% probability level. Hydrogen atoms and minor parts are omitted for clarity. n.d. = not detected (below LCMS detection limit in reaction mixture).

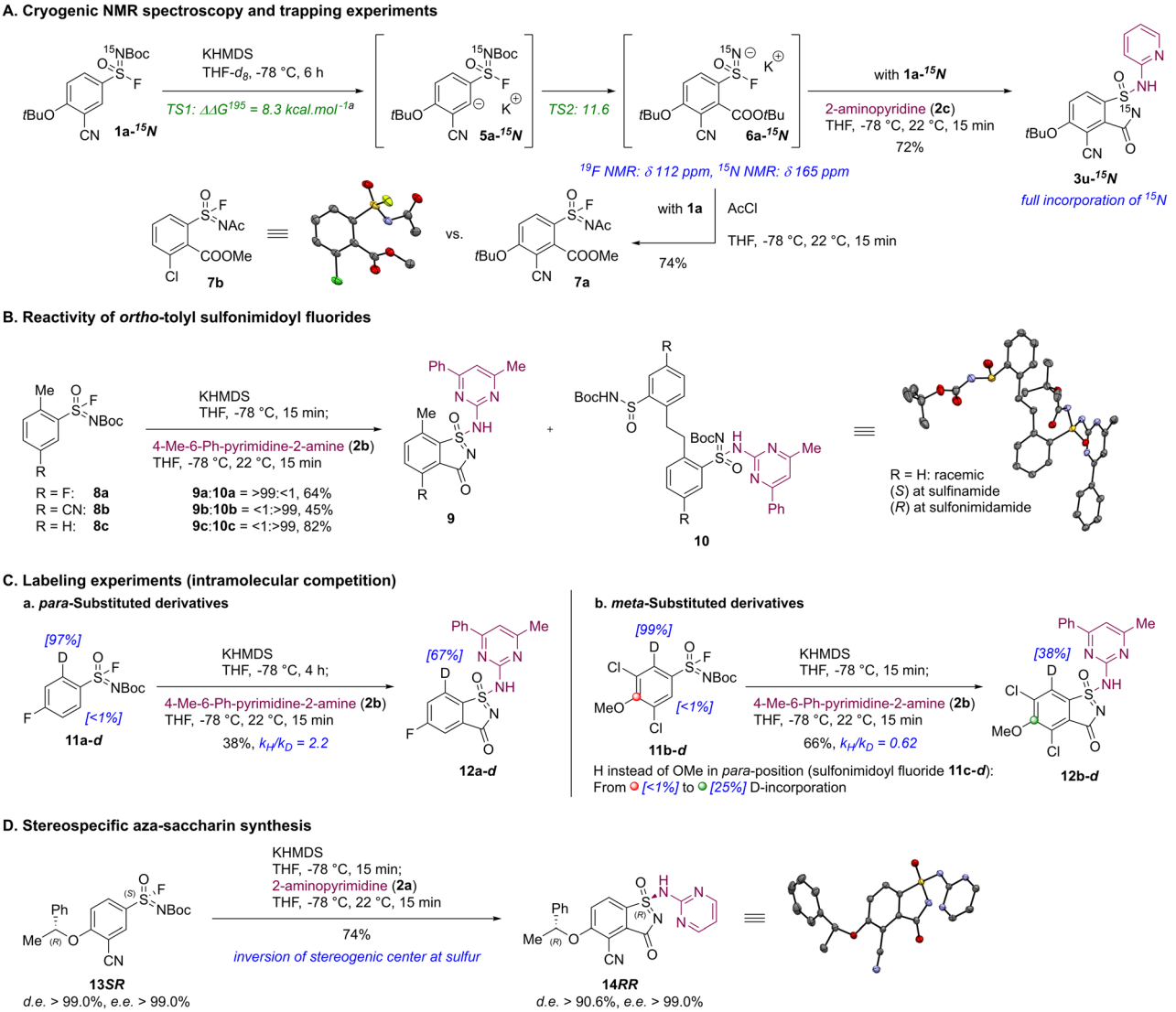

Scheme 4 Summary of mechanistic experiments for the formation of aza-saccharins. Reaction conditions: sulfonimidoyl fluoride (1 equiv.), KHMDS (2.00 equiv.), THF, −78 °C; 2-aminopyridine (**2c**, 1.20 equiv.), 4-Me-6-Ph-pyrimidine-2-amine (**2b**, 1.20 equiv.) or acyl chloride (6.00 equiv.), THF, −78 °C, 22 °C, 15 min. [a]Reaction profile for the KPA of unlabeled sulfonimidoyl fluoride **1a** was computed at the M06-2X/def2-TZVP level of theory with implicit solvent model (COSMO) for the treatment of THF. The relative Gibbs free energies $\Delta\Delta G^{195}$ are calculated at 195 K. Values correspond to isolated yields. Displacement ellipsoids are drawn at the 30% and 50% probability level. Hydrogen atoms and minor parts are omitted for clarity.

heterocycles delivered minor amounts of the pyrrole and indole aza-saccharins **3ay, 3az**, which could not be isolated, suggesting that these scaffolds may become accessible with further optimization.[30] The remaining N–H heteroaromatic nucleophiles tested were unreactive toward aza-saccharins **3ba–3bd**, indicating that hydrolysis, observed during LCMS analysis rather than under experimental conditions, predominantly accounted for most reactions.[20,31] Taken together, these observations underscore a limitation of the current protocol for these classes of nitrogen nucleophiles.

Mechanistic studies

A set of mechanistic experiments was conducted to support our mechanistic rationale in the KPA of aryl sulfonimidoyl fluorides prior to the addition of amines. Based on the observed regioselectivities and substituent-dependent reactivity trends, we postulated that inductive electron-withdrawing groups acidify the *ortho*-hydrogen atom adjacent to the sulfonimidoyl fluoride moiety, leading to the formation of the carbanionic intermediate **5a** upon deprotonation with KHMDS (Scheme 4A).[32,33] Rapid [1,4] Fries-type rearrangement *via* carbonyl migration within carbanion **5a** would yield cryogenically stable aryl sulfonimidoyl fluoridate anion **6a**, whose presence was supported by distinct ^{19}F NMR (δ 112 ppm) and ^{15}N NMR (δ 165 ppm) shifts in cryogenic NMR experiments utilizing ^{15}N-labeled sulfonimidoyl fluoride **1a-*15N***. Treatment of intermediate **6a-*15N*** with 2-aminopyridine (**2c**) provided aza-saccharin **3u-*15N*** *via* SuFEx reaction and cyclization with full incorporation of the

^{15}N-atom at the endocyclic position, whereas trapping of unlabeled intermediate **6a** with acetyl chloride resulted in a clean *N*-acylation affording sulfonimidoyl fluoride **7a** (compare with X-ray crystal structure of crystalline sulfonimidoyl fluoride **7b**).[20]

Moderately acidic hydrogen atoms at benzylic positions *ortho* to the sulfonimidoyl fluoride were suspected to compete with deprotonation at the desired *ortho*-position, suppressing aza-saccharin formation (*e.g.*, *ortho*-tolyl, Scheme 4B). Among the substituents investigated, only a *meta*-fluoro substituent of sulfonimidoyl fluoride **8a** was acidifying enough to allow successful and selective aza-saccharin **9a** formation while potentially stabilizing the deprotonated sulfonimidoyl fluoride **8a** *via* negative hyperconjugation.[23d,e] Conversely, reactions involving the cyano and the unsubstituted derivative favored deprotonation at the benzylic position,[12d] forming sulfinamide/sulfonimidamide dimers **10b**, **10c**, respectively, as a mixture of stereoisomers.[34]

Kinetic isotope effect (KIE) experiments *via* intramolecular competition revealed a normal KIE in *para*-fluoro sulfonimidoyl fluoride **11a–*d*** toward aza-saccharin **12a–*d*** (Scheme 4Ca, $k_H/k_D = 2.2$). Its magnitude is consistent with a kinetically controlled, effectively irreversible deprotonation (carbon-hydrogen/deuterium bond cleavage) occurring in an asynchronous, rate-determining transition state followed by a rapid carbonyl migration.[35] In contrast, bis-*meta*-dichloro sulfonimidoyl fluoride **11b–*d*** exhibited an inverse KIE (Scheme 4Cb, $k_H/k_D = 0.62$) attributable to a pre-equilibrium isotope effect (EIE), in which a fast, reversible deprotonation precedes slower carbonyl migration, and therefore reflecting thermodynamic isotope partitioning in this pre-equilibrium rather than intrinsic bond cleavage kinetics. Consistent with these observations, density functional theory (DFT) calculations supported the substitution-dependent shift in the selectivity-determining step between *meta*- and *para*-substituted sulfonimidoyl fluorides.[20] Additional evidence includes hydrogen/deuterium scrambling at the *para*-position of bis-*meta*-dichloro sulfonimidoyl fluoride **11c-*d***, indicating dynamic KPA behavior and sensitivity to substituent acidification (Scheme 4Cb). The coexistence of an inverse KIE together with deuterium exchange at nominally nonreactive carbon-hydrogen sites for *meta*-substituted sulfonimidoyl fluorides implies an increased barrier to carbonyl migration relative to *ortho*-deprotonation, rendering the deprotonation step reversible (compare the reaction profile for sulfonimidoyl fluoride **1a**, Scheme 4A).[36]

During the exploration of chiral information preservation at the sulfur atom, stereoisomerically pure sulfonimidoyl fluoride **13*SR*** (d.e. > 99.0%, e.e. > 99.0%, (*S*)-configuration at sulfur atom) afforded the corresponding aza-saccharin **14*RR*** (d.e. > 90.6%, e.e. > 99.0%) without any erosion of optical activity of the benzylic stereogenic center (Scheme 4D).[20] More importantly, upon KPA of sulfonimidoyl fluoride **13*SR***, SuFEx capture by 2-aminopyrimidine (**2a**) occurred with inversion of the stereogenic center at the sulfur atom,[37] and therefore highlighted the suitability of this transformation for stereospecific protocols. Minor losses in stereoinformation can be attributed to the degenerative nucleophilic attack of solvated fluoride ions originating from the released potassium fluoride.[13c] All results obtained from the cryogenic NMR spectroscopy, trapping experiment (Scheme 4A) and the stereospecific route (Scheme 4D) collectively validate the fluoro substituent being attached and thus chiral information at the sulfur atom being conserved throughout the entire KPA of sulfonimidoyl fluorides, further expanding the utilization of this synthetic methodology.

Conclusions

In conclusion, we have developed a regioselective method for the synthesis of aza-saccharins from aryl sulfonimidoyl fluorides and amines. This transformation displays broad applicability, accommodating electronically diverse substrates bearing inductive electron-withdrawing substituents as well as a range of amine partners, while maintaining high functional group tolerance. Mechanistic studies are consistent with an anionic [1,4] Fries-type rearrangement under strongly basic conditions, in which regioselective *ortho*-deprotonation is followed by rapid carbonyl migration to low-temperature-persistent aryl sulfonimidoyl fluoridate anions, revealing a distinct and previously unexplored mode of reactivity in S(VI) and SuFEx chemistry. The involvement of these fluoridate anions is supported by cryogenic $^{19}F/^{15}N$ NMR studies of a ^{15}N-labeled substrate, interception by acylation with X-ray characterization of the resulting adduct, and complementary computational analysis. Notably, chiral information at the sulfur center is preserved during the rearrangement, and subsequent SuFEx-based amination proceeds stereospecifically with inversion at sulfur, enabling a controlled and predictable route to stereodefined aza-saccharins.

Overall, this work expands the synthetic and mechanistic understanding of sulfonimidoyl fluorides and establishes a reliable entry to functionalized aza-saccharins. Future studies will assess whether the present methodology can be extended to heteroaryl sulfonimidoyl fluorides and their corresponding aza-saccharins, as well as to carbon- and oxygen-based nucleophiles. Concurrently, ongoing work in our laboratories is focused on investigating the physicochemical and pharmacokinetic properties of aza-saccharins and evaluating their potential as bioisosteric replacements for sulfonamides in medicinal chemistry, agrochemistry, and related disciplines.

Author contributions

M. L., L. P., M. E., J. J. M., M. S., C. Gatti, H. S., T. L. and R. J. performed the experiments, O. D. P., R. J. L., M. P., L. M. v. S., V. S. and I. A. carried out analytical characterizations, K. K. performed computational simulations, M. L., J. J. M. and P.-O. N. elaborated the reaction mechanism, and M. L., H. S., R. G., S. J. F., C. Gardelli and W. C. contributed to project planning and supervision.

Conflicts of interest

The authors declare the following competing financial interest(s): M. L., M. E., O. D. P., K. K., R. J. L., J. J. M., M. P., L. M. v. S., V. S., I. A., M. S., C. Gatti, H. S., R. J., R. G., S. J. F.,

C. Gardelli, P.-O. N. and W. C. are employees of AstraZeneca and may own stock or stock options. The authors have no other relevant affiliations or financial conflicts with the subject matter discussed in the manuscript apart from those disclosed. L. P. and T. L. and declare no conflict of interest.

Data availability

CCDC 2517062–2517074 contain the supplementary crystallographic data for this paper.[38a–m]

All experimental and computational data supporting the findings of this study are provided in the supplementary information (SI). Supplementary information: experimental procedures, NMR spectra, computational methods, and optimized geometries. See DOI: https://doi.org/10.1039/d6sc00432f.

Acknowledgements

The authors thank Dr. Yantao Chen (AstraZeneca, Sweden) and Dr. Igor Shamovsky (AstraZeneca, Sweden) for mechanistic discussions regarding the synthesis of sulfonimidamide derivatives, including aza-saccharins, and Prof. Dr. Magnus J. Johansson for proofreading the manuscript. L. P. and T. L. thank the Erasmus program, L. P. the Alsace region, and T. L. the Occitanie region for financial support during their internship stays at AstraZeneca, Sweden.

Notes and references

1 For different strategies regarding the synthesis of acyclic sulfonimidamides, see: (*a*) C. Liang, F. Robert-Peillard, C. Fruit, P. Müller, R. H. Dodd and P. Dauban, *Angew. Chem., Int. Ed.*, 2006, **45**, 4641–4644; (*b*) C. Liang, F. Collet, F. Robert-Peillard, P. Müller, R. H. Dodd and P. Dauban, *J. Am. Chem. Soc.*, 2008, **130**, 343–350; (*c*) C. Worch, I. Atodiresei, G. Raabe and C. Bolm, *Chem. Eur J.*, 2010, **16**, 677–683; (*d*) Y. Chen and J. Gibson, *RSC Adv.*, 2015, **5**, 4171–4174; (*e*) J. Buendia, G. Grelier, B. Darses, A. G. Jarvis, F. Taran and P. Dauban, *Angew. Chem., Int. Ed.*, 2016, **55**, 7530–7533; (*f*) F. Izzo, M. Schäfer, R. Stockmann and U. Lücking, *Chem.–Eur. J.*, 2017, **23**, 15189–15193; (*g*) T. Q. Davies, A. Hall and M. C. Willis, *Angew. Chem., Int. Ed.*, 2017, **56**, 14937–14941; (*h*) M. Wright, C. Martínez-Lamenca, J. E. Leenaerts, P. E. Brennan, A. A. Trabanco and D. Oehlrich, *J. Org. Chem.*, 2018, **83**, 9510–9516; (*i*) H. Yu, Z. Li and C. Bolm, *Angew. Chem., Int. Ed.*, 2018, **57**, 15602–15605; (*j*) E. L. Briggs, A. Tota, M. Colella, L. Degennaro, R. Luisi and J. A. Bull, *Angew. Chem., Int. Ed.*, 2019, **58**, 14303–14310; (*k*) M. Bremerich, C. M. Conrads, T. Langletz and C. Bolm, *Angew. Chem., Int. Ed.*, 2019, **58**, 19014–19020; (*l*) P. K. Chinthakindi, A. Benediktsdottir, P. I. Arvidsson, Y. Chen and A. Sandström, *Eur. J. Org Chem.*, 2020, 3796–3807; (*m*) T. Q. Davies, M. J. Tilby, J. Ren, N. A. Parker, D. Skolc, A. Hall, F. Duarte and M. C. Willis, *J. Am. Chem. Soc.*, 2020, **142**, 15445–15453; (*n*) G. B. Craven, E. L. Briggs, C. M. Zammit, A. McDermott, S. Greed, D. P. Affron, C. Leinfellner, H. R. Cudmore, R. R. Tweedy, R. Luisi, J. A. Bull and A. Armstrong, *J. Org. Chem.*, 2021, **86**, 7403–7424; (*o*) P. K. Tony and M. C. Willis, *J. Am. Chem. Soc.*, 2021, **143**, 15576–15581; (*p*) M. J. Tilby, D. F. Dewez, A. Hall, C. M. Lamenca and M. C. Willis, *Angew. Chem., Int. Ed.*, 2021, **60**, 25680–25687; (*q*) G.-f. Yang, Y. Yuan, Y. Tian, S.-q. Zhang, X. Cui, B. Xia, G.-x. Li and Z. Tang, *J. Am. Chem. Soc.*, 2023, **145**, 5439–5446; (*r*) D.-D. Liang, N. Lional, B. Scheepmaker, M. Subramaniam, G. Li, F. M. Miloserdov and H. Zuilhof, *Org. Lett.*, 2023, **25**, 5666–5670; (*s*) J. A. Andrews, J. Kalepu, C. F. Palmer, D. L. Poole, K. E. Christensen and M. C. Willis, *J. Am. Chem. Soc.*, 2023, **145**, 21623–21629; (*t*) S. Pan, F. F. Mulks, P. Wu, K. Rissanen and C. Bolm, *Angew. Chem., Int. Ed.*, 2024, **63**, e202316702; (*u*) P. R. Athawale, Z. P. Shultz, A. Saputo, Y. D. Hall and J. M. Lopchuk, *Nat. Commun.*, 2024, **15**, 7001; (*v*) S. Teng, Z. P. Shultz, C. Shan, L. Wojtas and J. M. Lopchuk, *Nat. Chem.*, 2024, **16**, 183–192; (*w*) P. Wu, L. Ling, Y. Hu, S. Pan and C. Bolm, *ACS Sustainable Chem. Eng.*, 2024, **12**, 15875–15880; (*x*) D. Deans, S. Iqbal, Z. Zhong, C. S. Begg, N. A. Anderson, S. Ferrer Cabrera and J. A. Bull, *ChemistryEurope*, 2025, **3**, e202500163.

2 For the synthesis of cyclic sulfonimidamides, see: (*a*) B. E. Cathers and J. V. Schloss, *Bioorg. Med. Chem. Lett.*, 1999, **9**, 1527–1532; (*b*) N. Pemberton, H. Graden, E. Evertsson, E. Bratt, M. Lepistö, P. Johannesson and P. H. Svensson, *ACS Med. Chem. Lett.*, 2012, **3**, 574–578; (*c*) I. Sen, D. P. Kloer, R. G. Hall and S. Pal, *Synthesis*, 2013, **45**, 3018–3028; (*d*) P. K. Chinthakindi, A. Benediktsdottir, A. Ibrahim, A. Wared, C.-J. Aurell, A. Pettersen, E. Zamaratski, P. I. Arvidsson, Y. Chen and A. Sandström, *Eur. J. Org Chem.*, 2019, 1045–1057; (*e*) Y. Chen, J. Söderlund, G. Grönberg, A. Pettersen and C.-J. Aurell, *Eur. J. Org Chem.*, 2019, 4731–4740; (*f*) A.-K. Bachon, A. Hermann and C. Bolm, *Chem.–Eur. J.*, 2019, **25**, 5889–5892; (*g*) J.-H. Schöbel, M. T. Passia, N. A. Wolter, R. Puttreddy, K. Rissanen and C. Bolm, *Org. Lett.*, 2020, **22**, 2702–2706; (*h*) J.-H. Schöbel, W. Liang, D. Wöll and C. Bolm, *J. Org. Chem.*, 2020, **85**, 15760–15766; (*i*) J.-H. Schöbel, P. Elbers, K.-N. Truong, K. Rissanen and C. Bolm, *Adv. Synth. Catal.*, 2021, **363**, 1322–1329; (*j*) F. Krauskopf, K.-N. Truong, K. Rissanen and C. Bolm, *Org. Lett.*, 2021, **23**, 2699–2703; (*k*) P. Wu, J. S. Ward, K. Rissanen and C. Bolm, *Adv. Synth. Catal.*, 2023, **365**, 522–526; (*l*) K. Natarajan, S. Ravindra, V. R. P. Priya, R. Kataria and G. C. Nandi, *Eur. J. Org Chem.*, 2024, **27**, e202301217; (*m*) T. Guo, L. Xu and J. Dong, *Org. Lett.*, 2025, **27**, 1356–1361.

3 For reviews on the synthesis and applications of sulfonimidamides, see: (*a*) P. K. Chinthakindi, T. Naicker, N. Thota, T. Govender, H. G. Kruger and P. I. Arvidsson, *Angew. Chem., Int. Ed.*, 2017, **56**, 4100–4109; (*b*) G. C. Nandi and P. I. Arvidsson, *Adv. Synth. Catal.*, 2018, **360**, 2976–3001; (*c*) M.-K. Wei and M. C. Willis, *Synthesis*, 2025, **57**, 1429–1440.

4 For examples of sulfonimidamide inhibitors in NOD-like receptor, pyrin domain-containing protein (NLRP)-

associated disorders, see: (*a*) J. Katz, W. Roush, H. M. Seidel, D.-M. Shen and S. Venkatraman, *WO2020154499 A1*, 2020; (*b*) P. Gibbons, K. W. Lai, C. Nilewski, R. M. Pastor, S. T. Staben, C. Stivala, B.-Y. Zhu and H. Chen , *WO2021150574 A1*, 2021; (*c*) K. W. Lai, C. Nilewski, R. M. Pastor and C. Stivala, *WO2023004257 A1*, 2023; (*d*) D.-M. Shen, K. F. Byth, D. Bertheloot, S. Braams, S. Bradley, D. Dean, *et al.*, *J. Med. Chem.*, 2025, **68**, 5529–5550.

5 For a patent example of sulfonimidamide inhibitors in Stimulator of Interferon Genes (STING)-associated disorders, see: S. Venkatraman, W. R. Roush and H. M. Seidel, WO2020106736 A1, 2020.

6 For a patent example of sulfonimidamide inhibitors in Liver X Receptor (LXR)-associated disorders, see: C. Gege, M. Birkel, E. Hambruch, U. Deuschle and C. Kremoser, WO2018188795 A1, 2018.

7 For a patent example of sulfonimidamides in pesticidal applications, see: I. Sen, V. Sikervar, G. Rawal, A. Edmunds, S. Rendler, M. Muehlebach and D. Emery, WO2019076778 A1, 2019.

8 This class of aza-saccharins was referred to as "cluster D", see: Y. Chen, C.-J. Aurell, A. Pettersen, R. J. Lewis, M. A. Hayes, M. Lepistö, A. C. Jonson, H. Leek and L. Thunberg, *ACS Med. Chem. Lett.*, 2017, **8**, 672–677.

9 For patent examples of aza-saccharins as NLRP3 modulators, see: (*a*) J. Katz, W. Roush, H. M. Seidel, D.-M. Shen and S. Venkatraman, *WO2020102100 A1*, 2020; (*b*) E. Gabellieri and J. Molette, *WO2020254697 A1*, 2020.

10 For a perspective regarding NLRP3 modulators mentioning aza-saccharins, see: N. Li, R. Zhang, M. Tang, M. Zhao, X. Jiang, X. Cai, N. Ye, K. Su, J. Peng, X. Zhang, W. Wu and H. Ye, *J. Med. Chem.*, 2023, **66**, 14447–14473.

11 For examples regarding an anionic [1,4] Fries-type rearrangement, see: (*a*) H. Kim, K. Inoue and J.-i. Yoshida, *Angew. Chem., Int. Ed.*, 2017, **56**, 7863–7866; (*b*) M. Korb and H. Lang, *Chem. Soc. Rev.*, 2019, **48**, 2829–2882.

12 For examples regarding regioselective Fries rearrangement, including directed Snieckus-Fries rearrangement, see: (*a*) K. J. Singh and D. B. Collum, *J. Am. Chem. Soc.*, 2006, **128**, 13753–13760; (*b*) K. Groom, S. M. S. Hussain, J. Morin, C. Nilewski, T. Rantanen and V. Snieckus, *Org. Lett.*, 2014, **16**, 2378–2381; (*c*) Y. Ma, R. A. Woltornist, R. F. Algera and D. B. Collum, *J. Org. Chem.*, 2019, **84**, 9051–9057; (*d*) S. Ghinato, F. De Nardi, P. Bolzoni, A. Antenucci, M. Blangetti and C. Prandi, *Chem. Eur J.*, 2022, **28**, e202201154.

13 For the synthesis of sulfonimidoyl fluorides, see: (*a*) C. R. Johnson, K. G. Bis, J. H. Cantillo, N. A. Meanwell, M. F. D. Reinhard, J. R. Zeller and G. P. Vonk, *J. Org. Chem.*, 1983, **48**, 1–3; (*b*) B. Gao, S. Li, P. Wu, J. E. Moses and K. B. Sharpless, *Angew. Chem., Int. Ed.*, 2018, **57**, 1939–1943; (*c*) S. Greed, E. L. Briggs, F. I. M. Idiris, A. J. P. White, U. Lücking and J. A. Bull, *Chem. Eur J.*, 2020, **26**, 12533–12538; (*d*) L. Wang and J. Cornella, *Angew. Chem., Int. Ed.*, 2020, **59**, 23510–23515; (*e*) Y. Liu, Q. Pan, X. Hu, Y. Guo, Q.-Y. Chen and C. Liu, *Org. Lett.*, 2021, **23**, 3975–3980; (*f*) A. Zogu, K. Ullah, S. Spanopoulos, E. Ismalaj, W. M. De Borggraeve and J. Demaerel, *Angew. Chem., Int. Ed.*, 2024, **63**, e202403797; (*g*) M. Andresini, L. Marraffa, D. Serbetci, P. Natho, M. Colella, L. Degennaro and R. Luisi, *Adv. Synth. Catal.*, 2025, **367**, e202400908; (*h*) H.-s. Huang, Y. Yuan, W. Wang, S.-q. Zhang, X.-k. Nie, W.-t. Yang, X. Cui, Z. Tang and G.-x. Li, *Angew. Chem., Int. Ed.*, 2025, **59**, e202415873.

14 For a successful example using KHMDS as a base in a Fries rearrangement, see: G. M. R. Boston, I. Frank and H. Butenschön, *Helv. Chim. Acta*, 2021, **104**, e2100025.

15 An average recovery rate of 90% was determined for the preparative liquid chromatography purification. Isolated yields are reported uncorrected.

16 For the complete solvent screen data, including different ethers and toluene, together with corresponding LCMS yields, see the SI.

17 LCMS analysis of the reaction mixture for the sulfonimidoyl chloride analogue of sulfonimidoyl fluoride **1a** was dominated by low-intensity and unassigned signals consistent with degradation, which precluded meaningful quantitation. Accordingly, Table 1 reports "degradation" and no LCMS yield was determined (*cf.* ref. 2*d* for a direct conversion of sulfonimidoyl chlorides with nitrogen nucleophiles).

18 The increased side product formation observed for the Moc analogue of sulfonimidoyl fluoride **1a** is consistent with competitive nucleophilic reactions by the released methanolate anion under the reaction conditions. Although other carbamate protecting groups (e.g., benzyloxycarbonyl (Cbz), 9-fluorenylmethyoxycarbonyl (Fmoc), allyloxycarbonyl (Alloc)) were not examined, the Boc vs. Moc comparison, together with established nucleophilicity trends of carbamate-derived alkoxides in aprotic media, suggests that carbamates releasing alkoxides more nucleophilic than the Boc-derived *tert*-butanolate would likely promote analogous side reactions. Consequently, Boc was selected as the optimal protecting group. For nucleophilicity trends of alkoxides, especially between methanolate and *tert*-butanolate, see: (*a*) D. K. Bohme and L. B. Young, *J. Am. Chem. Soc.*, 1970, **92**, 7354–7358; (*b*) J. M. Dust and E. Buncel, *Can. J. Chem.*, 1991, **69**, 978–986.

19 NaHMDS was found to activate only certain sulfonimidoyl fluorides, such as sulfonimidoyl fluoride **1a**. NaHMDS was proven to be inefficient in the activation of *para*-bromo sulfonimidoyl fluoride **1i**.

20 See the SI for details.

21 For studies regarding ion pairing, aggregation and/or metal–substrate coordination of alkali-metal silazide bases (LiHMDS, NaHMDS and KHMDS), see: (*a*) B. L. Lucht and D. B. Collum, *J. Am. Chem. Soc.*, 1995, **117**, 9863–9874; (*b*) R. A. Woltornist and D. B. Collum, *J. Org. Chem.*, 2021, **86**, 2406–2422; (*c*) J. A. Spivey and D. B. Collum, *J. Am. Chem. Soc.*, 2024, **146**, 17827–17837.

22 Side product formation in the KPA of sulfonimidoyl fluorides generally started at temperatures above −50 °C.

23 For general trends regarding inductive effects, polarization, and stereoelectronic effects (hyperconjugative acceptor ability of σ-bonds) in substituted phenyl carbanions, see: (*a*) P. G. Wenthold and R. R. Squires, *J. Mass Spectrom.*, 1995, **30**, 17–24; (*b*) P. B. M. Andrade and J. M. Riveros, *J. Mass Spectrom.*, 1996, **31**, 767–770; (*c*) I. V. Alabugin and T. A. Zeidan, *J. Am. Chem. Soc.*, 2002, **124**, 3175–3185; (*d*) Z. Tian and S. R. Kass, *Chem. Rev.*, 2013, **113**, 6986–7010; (*e*) I. V. Alabugin, in, *Stereoelectronic Effects: A Bridge Between Structure and Reactivity*, John Wiley & Sons, 2016, pp. 214–235.

24 The relative ranking of the sulfonimidoyl fluoride (SOFNBoc) group is based on experiments with the 3,5-difluoro and 3,5-dichloro sulfonimidoyl fluoride derivatives. While the aza-saccharin formation with the 3,5-difluoro sulfonimidoyl fluoride derivative was unproductive, the corresponding aza-saccharin was isolated in 61% yield under the use of the 3,5-dichloro sulfonimidoyl fluoride derivative.

25 X-ray crystal structures of aza-saccharins **3n–3r** derived from bis-*meta*-substituted sulfonimidoyl fluorides are provided in the Supporting Information and support the corresponding regioselectivity assignments.

26 For the reactivity and regioselectivity in the deprotonation of substituted arenes with the Lochmann-Schlosser base, see: (*a*) G. Katsoulos, S. Takagishi and M. Schlosser, *Synlett*, 1991, 731–732; (*b*) E. Marzi, F. Mongin, A. Spitaleri and M. Schlosser, *Eur. J. Org Chem.*, 2001, 2911–2915; (*c*) E. Marzi, A. Spitaleri, F. Mongin and M. Schlosser, *Eur. J. Org Chem.*, 2002, 2508–2517; (*d*) E. Marzi, J. Gorecka and M. Schlosser, *Synthesis*, 2004, 1609–1614; (*e*) M. Schlosser, *Angew. Chem., Int. Ed.*, 2005, **44**, 376–393.

27 For a review on the directed *ortho*-metalation with lithium bases, see: V. Snieckus, *Chem. Rev.*, 1990, **90**, 879–933.

28 The unsubstituted phenyl derivative gave trace conversion under standard conditions, however, aza-saccharin **3m** was obtained in low yield upon temperature adjustment during KPA. For the 4-methoxy derivative, minor formation of aza-saccharin **3s** was detected via LCMS analysis following KPA at −30 °C for 30 min, yet the product could not be isolated.

29 A modified synthetic protocol was evaluated for aza-saccharin formation with aliphatic amines using catalytic amounts of 1-hydroxybenzotriazole (HOBt), however, no improvements in isolated yields were observed (*cf.* ref. 1*x*).

30 Attempts to increase conversion toward aza-saccharins **3ay**, **3az** by longer reaction times and/or warming to 40 °C led to increased side product formation.

31 A detailed summary of the additional nitrogen nucleophile screening experiments, including LCMS observations and side product profiles, is provided in the SI.

32 For KHMDS acting both as a base and single-electron donor, see: N. Ogawa, Y. Yamaoka, K.-i. Yamada and K. Takusa, *Org. Lett.*, 2017, **19**, 3327–3330.

33 Electron paramagnetic resonance (EPR) spectroscopy did not reveal any radical intermediates in the KPA of sulfonimidoyl fluoride **1a**.

34 Corresponding 6-membered ring products could not be detected via LCMS analysis of the reaction mixture with sulfonimidoyl fluorides **8b**, **8c**, respectively. Their formation would theoretically occur via benzylic deprotonation, followed by an anionic [1,5] Fries-type rearrangement and analogous interception by amines to effect ring closure (*cf.* ref. 12*d* for a related anionic [1,4] Fries rearrangement).

35 For kinetic isotope effect (KIE) experiments via intramolecular competition, see: (*a*) E. M. Simmons and J. F. Hartwig, *Angew. Chem., Int. Ed.*, 2012, **51**, 3066–3072; (*b*) W. Zi, Y.-M. Wang and F. D. Toste, *J. Am. Chem. Soc.*, 2014, **136**, 12864–12867; (*c*) Z. Mao and C. T. Campbell, *ACS Catal.*, 2020, **10**, 4181–4192.

36 For examples of kinetic isotope effects used to elucidate reaction mechanisms, including inverse kinetic isotope effects and pre-equilibrium isotope effects, see: (*a*) D. G. Churchill, K. E. Janak, J. S. Wittenberg and G. Parkin, *J. Am. Chem. Soc.*, 2003, **125**, 1403–1420; (*b*) M. Gomez-Gallego and M. A. Sierra, *Chem. Rev.*, 2011, **111**, 4857–4963; (*c*) X. Gao, X.-Y. Yu and C.-R. Chang, *Phys. Chem. Chem. Phys.*, 2022, **24**, 15182–15194.

37 For stereospecific substitution at chiral S(VI) centers (including sulfonimidoyl fluorides), which is commonly consistent with an S_N2-type displacement leading to inversion at sulfur, see: (*a*) S. Greed, O. Symes and J. A. Bull, *Chem. Commun.*, 2022, **58**, 5387–5390; (*b*) O. L. Symes and J. A. Bull, *Org. Chem. Front.*, 2025, **12**, 6681–6697.

38 (*a*) CCDC 2517062: Experimental Crystal Structure Determination, 2026, DOI: 10.5517/ccdc.csd.cc2qh6k0; (*b*) CCDC 2517063: Experimental Crystal Structure Determination, 2026, DOI: 10.5517/ccdc.csd.cc2qh6l1; (*c*) CCDC 2517064: Experimental Crystal Structure Determination, 2026, DOI: 10.5517/ccdc.csd.cc2qh6m2; (*d*) CCDC 2517065: Experimental Crystal Structure Determination, 2026, DOI: 10.5517/ccdc.csd.cc2qh6n3; (*e*) CCDC 2517066: Experimental Crystal Structure Determination, 2026, DOI: 10.5517/ccdc.csd.cc2qh6p4; (*f*) CCDC 2517067: Experimental Crystal Structure Determination, 2026, DOI: 10.5517/ccdc.csd.cc2qh6q5; (*g*) CCDC 2517068: Experimental Crystal Structure Determination, 2026, DOI: 10.5517/ccdc.csd.cc2qh6r6; (*h*) CCDC 2517069: Experimental Crystal Structure Determination, 2026, DOI: 10.5517/ccdc.csd.cc2qh6s7; (*i*) CCDC 2517070: Experimental Crystal Structure Determination, 2026, DOI: 10.5517/ccdc.csd.cc2qh6t8; (*j*) CCDC 2517071: Experimental Crystal Structure Determination, 2026, DOI: 10.5517/ccdc.csd.cc2qh6v9; (*k*) CCDC 2517072: Experimental Crystal Structure Determination, 2026, DOI: 10.5517/ccdc.csd.cc2qh6wb; (*l*) CCDC 2517073: Experimental Crystal Structure Determination, 2026, DOI: 10.5517/ccdc.csd.cc2qh6xc; (*m*) CCDC 2517074: Experimental Crystal Structure Determination, 2026, DOI: 10.5517/ccdc.csd.cc2qh6yd.